Inorg. Chem. **2005**, *44*, 5011–5020

Unexpected Ferromagnetic Interaction in a New Tetranuclear Copper(II) Complex: Synthesis, Crystal Structure, Magnetic Properties, and Theoretical Studies

Matilde Fondo,*,† Ana M. García-Deibe,† Monstserrat Corbella,‡ Eliseo Ruiz,‡ Javier Tercero,‡ Jesús Sanmartín,§ and Manuel R. Bermejo§

Departamento de Química Inorgánica, Facultade de Ciencias, Universidade de Santiago de Compostela, E-27002 Lugo, Spain, Departament de Química Inorgánica, Facultat de Química, Universitat de Barcelona, E-08028 Barcelona, Spain, and Departamento de Química Inorgánica, Facultade de Química, Universidade de Santiago de Compostela, E-15782 Santiago de Compostela, Spain

Received December 9, 2004

The new tetranuclear carbonate complex $[Cu_2L)_2(CO_3)]\cdot 8H_2O$ (**1**·$8H_2O$) (H_3L = (2-(2-hydroxyphenyl)-1,3-bis[4-(2-hydroxyphenyl)-3-azabut-3-enyl]-1,3-imidazolidine) has been obtained by two different synthetic routes and fully characterized. Recrystallization of **1**·$8H_2O$ in methanol yields single crystals of $\{[(Cu_2L)_2(CO_3)]\}_2\cdot 12H_2O$ (**1**·$6H_2O$), suitable for X-ray diffraction studies. The crystal structure of **1**·$6H_2O$ shows two crystallographically different tetranuclear molecules in the asymmetric unit, **1a** and **1b**. Both molecules can be understood as self-assembled from two dinuclear $[Cu_2L]^+$ cations, joined by a μ_4-η^2:η^1:η^1 carbonate ligand. The copper atoms of each crystallographically different $[(Cu_2L)_2(CO_3)]$ molecule present miscellaneous coordination polyhedra: in both **1a** and **1b**, two metal centers are in square pyramidal environments, one displays a square planar chromophore and the other one has a geometry that can be considered as an intermediate between square pyramid and trigonal bipyramid. Magnetic studies reveal net intramolecular ferromagnetic coupling between the metal atoms. Density functional calculations allow the assignment of the different magnetic coupling constants and explain the unexpected ferromagnetic behavior, because of the presence of an unusual NCN bridging moiety and countercomplementarity of the phenoxo (or carbonate) and NCN bridges.

Introduction

The carbonate anion itself is a versatile bridging ligand, which may adopt various binding modes, to generate complexes of different nuclearity.[1−6] Copper(II) carbonate coordination chemistry has recently received particular attention, with inspiration drawn from such disparate fields as bioinorganic chemistry[6−11] and/or the relationship between the bridging modes of the carbonate ligand and the magnetic properties.[12−19]

* To whom correspondence should be addressed. E-mail: qimatf69@usc.es.

† Departamento de Química Inorgánica, Facultade de Ciencias, Universidade de Santiago de Compostela.

‡ Departament de Química Inorgánica, Universitat de Barcelona.

§ Departamento de Química Inorgánica, Facultade de Química, Universidade de Santiago de Compostela.

(1) Einstein, F. W. B.; Willis, A. C. *Inorg. Chem.* **1981**, *20*, 609.
(2) Palmer, D. A.; Van Eldik, R.; *Chem. Rev.* **1983**, *83*, 651.
(3) Mak, T. C. W.; Li, P.; Zheng, C.; Huang,K.; *J. Chem. Soc., Chem. Commun.* **1986**, 1597.
(4) Alvarez, R.; Atwood, J. L.; Carmona, E.; Perez, Poveda, M. L.; Rogers, R. D. *Inorg. Chem.* **1991**, *30*, 1493.
(5) Escuer, A.; Vicente, R.; Kumar, S. B.; Solans, X.; Font-Badía, M. J.; Caneschi, A. *Inorg. Chem.* **1996**, *35*, 3094.
(6) Bode, R. H.; Driesden, W. L.; Hulsbergen, F. B.; Reedijk, J.; Spek, A. L. *Eur. J. Inorg. Chem.* **1999**, 505.
(7) Kitajima, N.; Hikichi, S.; Tanaka, M.; Moro-oka, Y. *J. Am. Chem. Soc.* **1993**, *115*, 5496.
(8) Bazzicalupi, C.; Bencini, A.; Bianchi, A.; Fursi, V.; Paoletti, P.; Valtancoli, B. *J. Chem. Soc., Chem. Commun.* **1995**, 1555.
(9) *Comprehensive Biological Catalysis. A Mechanistic Reference*; Sinnot, M., Ed.; Academic Press: San Diego, CA, 1998; Vol. I−IV.
(10) Fernandes, C.; Neves, A.; Bortoluzzi, A. J.; Szpoganicz B.; Schwingel, E. *Inorg. Chem. Commun.* **2001**, *4*, 354.
(11) Mao,Z−W.; Heinemann, F. W.; Liehr, G.; van Eldik, R. *J. Chem. Soc., Dalton Trans.* **2001**, 3652.
(12) Escuer, A.; Peñalba, E.; Vicente, R.; Solans, X.; Font-Badía, M. J. *J. Chem. Soc., Dalton Trans.* **1997**, 2315.
(13) Escuer, A.; Mautner, F. A.; Peñalba, E.; Vicente, R. *Inorg. Chem.* **1998**, *37*, 4190 and references therein.
(14) Nishida, Y.; Yatani, A.; Taka, J.-I.; Kashino, S.; Mori, W.; Suzuki, S. *Chem. Lett.* **1999**, 135.

10.1021/ic0482741 CCC: $30.25
Published on Web 06/14/2005

Scheme 1

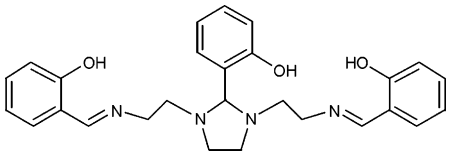

The magnetic behavior of the dinuclear copper carbonate complexes is the best understood among those of polynuclear carbonate compounds. In fact, higher nuclearities are less common and tetranuclear copper carbonate complexes are still scarce in the literature. To the best of our knowledge, only four μ_4-η^2:η^1:η^1 carbonate copper compounds have been crystallographically characterized,[1,12,17] three of which were magnetically studied, and they show a net antiferromagnetic coupling.[12,17]

Additionally, dinuclear Cu(II) complexes with two phenoxo bridging ligands are widely reported in the literature. This kind of compound frequently shows square pyramid geometry around the copper atoms and a strong antiferromagnetic coupling. By contrast, few compounds showing only one phenoxo bridging ligand have been described.[20−25] Recently, we have reported[26] the dinuclear copper complexes $[Cu_2L(AcO)]$[26a] and $[Cu_2L(OMe)]$,[26b] with the heptadentate Schiff base ligand H_3L depicted in Scheme 1. In these compounds, the Cu(II) ions are bridged by the central phenoxo group of the Schiff base and by an external acetate or methanolate ligand, and they show an overall ferromagnetic coupling.

In this work, we describe a new Cu(II) complex with the same H_3L heptadentate Schiff base ligand. In this case study, a tetranuclear complex containing carbonate and phenoxo groups functioning as bridging ligands was isolated. Its synthesis, crystal structure, and magnetic properties are studied. Because of the unusual ferromagnetic coupling observed, DFT calculations were carried out in order to explain the origin of this apparent anomalous behavior.

(15) Sertucha, J.; Luque, A.; Román, P.; Lloret, F.; Julve, M. *Inorg. Chem. Commun.* **1999**, *2*, 14.
(16) van Albada, G. A.; Mutikainen, I.; Roubeau, O. S.; Turpeinen, U.; Reedijk, J. *Eur. J. Inorg. Chem.* **2000**, 2179.
(17) Rodríguez, M.; LLobet, A.; Corbella, M.; Müller, P.; Usón, M. A.; Martell, A. E.; Reibenspens, J. *J. Chem. Soc., Dalton Trans.* **2002**, 2900.
(18) Kruger, P. E.; Fallon, G. D.; Moubaraki, B.; Berry, K. J.; Murray, K. S. *Inorg. Chem.* **1995**, *34*, 8.
(19) van den Brenk, A. L.; Byriel, K. A.; Fairlie, D. P.; Gahan, R. L.; Hanson, G. R.; Hawkins, C. J.; Jones, A.; Kennard, C. H. L.; Moubaraki, B.; Murray, K. S. *Inorg. Chem.* **1994**, *33*, 3549.
(20) Berends, H. P.; Stephan, D. W. *Inorg. Chem.* **1987**, *26*, 749.
(21) Nishida, Y.; Shimo, H.; Maehara, H.; Kida, S. *J. Chem. Soc., Dalton Trans.* **1985**, 1945.
(22) Holz, R. C.; Brink, J. M.; Gobena, F. T.; O'Connor, C. J. *Inorg. Chem.* **1994**, *33*, 6086.
(23) Holz, R. C.; Bradshaw, J. M.; Bennett, B. *Inorg. Chem.* **1998**, *37*, 1219.
(24) Bertoncello, K.; Fallon, G. D.; Hodgkin, J. H.; Murray, K. S. *Inorg. Chem.* **1988**, *27*, 4750.
(25) Handa, M.; Takemoto, T.; Thompson, L. K.; Mikuriya, M.; Ikemi, S.; Lim, J.-W.; Sugimori, T.; Iromitsu, I.; Kasuga, K. *Chem. Lett.* **2001**, 316.
(26) (a) Fondo, M.; García-Deibe, A. M.; Sanmartín, J.; Bermejo, M. R.; Lezama, L.; Rojo, T. *Eur. J. Inorg. Chem.* **2003**, 3703−3706. (b) Fondo, M.; García-Deibe, A. M.; Corbella, M.; Ribas, J.; Llamas-Saiz, A.; Bermejo, M. R.; Sanmartín, J. *J. Chem. Soc., Dalton Trans*, **2004**, 3503−3507.

Table 1. Crystal Data and Structure Refinement for $\mathbf{1}\cdot 6H_2O$

empirical formula	$C_{110}H_{128}N_{16}O_{30}Cu_8$
formula weight	2662.70
temperature (K)	293(2)
wavelength (Å)	0.71073
crystal system	triclinic
space group	*P-1*
a (Å)	14.202(4)
b (Å)	16.580(4)
c (Å)	25.376(7)
α (deg)	93.182(5)
β (deg)	104.313(4)
γ (deg)	92.762(5)
Z	2
absorption coefficient (mm^{-1})	1.528
crystal size (mm^3)	0.29 × 0.23 × 0.12
reflections collected	22931
independent reflections	22931
absorption correction	SADABS
data/restraints/parameters	22931/0/1513
final *R* indices [$I > 2\sigma(I)$]	$R_1 = 0.0772$, wR2 = 0.2117
R indices (all data)	$R_1 = 0.1243$, wR2 = 0.2380

Experimental Section

General Procedures. Elemental analysis of C, H, and N was performed on a Carlo Erba EA 1108 analyzer. The IR spectrum was recorded as a KBr pellet on a Bio-Rad FTS 135 spectrophotometer in the range 4000−600 cm^{-1}. The electrospray mass spectrum was obtained on a Hewlett-Packard LC/MS spectrometer in methanol as the solvent. A powder X-ray diffractogram of $\mathbf{1}\cdot 8H_2O$ was recorded at room temperature on a Siemens D5005 diffractometer using Cu Kα radiation ($\lambda = 1.5406$ Å).

Syntheses. H_3L (Scheme 1) and $[Cu_2L(OAc)]\cdot 6H_2O$ were obtained as previously described.[26a] All of the solvents and tetramethylammonium hydroxide pentahydrate are commercially available and were used without further purification.

$[(Cu_2L)_2(CO_3)]\cdot 8H_2O$ ($\mathbf{1}\cdot 8H_2O$) can be obtained by two different methods:

(1) Chemical Synthesis. $NMe_4OH\cdot 5H_2O$ (0.073 g, 0.40 mmol) was added to a methanol solution (20 mL) of $[Cu_2L(OAc)]\cdot 6H_2O$ (0.3 g, 0.40 mmol) in air. The mixture was stirred for 4 h, and the resultant green solution was filtered in a sintered glass funnel to eliminate any minimal impurity. Slow evaporation of the solution afforded green small crystals, which were filtered and dried in air. The analysis of the sample is in agreement with the $[(Cu_2L)_2(CO_3)]\cdot 8H_2O$ proposed stoichiometry. Yield: 0.15 g (55%). Anal. Calcd for $C_{55}H_{70}N_8O_{17}Cu_4$ (Found): C, 48.3 (48.3); H, 5.1 (5.3); N, 8.2 (8.3). MS *m*/*z* (+ES): 581.5 ($[Cu_2L]^+$). IR (cm^{-1}, KBr disk): 1535, 1342 ($\nu(CO_3)$), 1633 ($\nu(C{=}N)$, 3425 ($\nu(OH_2)$).

Crystals of $\{[(Cu_2L)_2(CO_3)]\}_2\cdot 12H_2O$ ($\mathbf{1}\cdot 6H_2O$) suitable for single X-ray diffraction studies were obtained by the slow evaporation of a dilute solution of $\mathbf{1}\cdot 8H_2O$ in methanol.

The same complex is obtained if acetonitrile instead of methanol is used as a solvent.

(2) Electrochemical Synthesis. An acetonitrile solution of H_3L (0.1 g, 0.218 mmol), containing ca. 10 mg of tetramethylammonium perchlorate, was electrolyzed at 10 mA, for 2 h 20 min, using a platinum wire as the cathode and a copper plate as the anode. The resulting green solution was filtered in a sintered glass funnel to eliminate the minimal possible impurity. Slow evaporation of the filtered solution yielded $\mathbf{1}\cdot 8H_2O$ as small crystals.

Single X-ray Crystallographic Measurements. Prism green crystals of $\mathbf{1}\cdot 6H_2O$, suitable for single-crystal X-ray studies, were obtained by slow evaporation of a methanol solution of $\mathbf{1}\cdot 8H_2O$. Crystal data and details of refinement are given in Table 1. Data were collected at 293 K on a Bruker SMART CCD-1000 diffrac-

tometer, employing graphite-monochromatic Mo Kα ($\lambda = 0.71073$ Å) radiation. Data were processed and corrected for Lorentz and polarization effects. A SADABS absorption correction was applied.[27] The structure was solved by direct methods and refined by full matrix least squares based on F^2, using the SHELX-97 program package.[28] Non-hydrogen atoms were anisotropically refined. Hydrogen atoms bonded to carbon were included in the structure factor calculation in idealized positions but not refined. Hydrogen attached to oxygen atoms were located in the Fourier map and included at these sites, with a fixed $U = 0.1$ Å^2, without further refinement.

Magnetic and Electron Paramagnetic Resonance (EPR) Measurements. Magnetic susceptibility measurements for crushed crystalline samples of **1**·8H_2O were carried out at the Servei de Magnetoquímica of the Universitat de Barcelona with a Quantum Design SQUID MPMS-XL susceptometer, working in the range of 2−300 K under magnetic fields of 500 G (2−37 K) and 10 000 G (2−300 K). Magnetization at 2 K was recorded between 0 and 50 000 G. Magnetic fields of 2500, 5000, 10 000, 20 000, and 30 000 G were used for magnetization measurements in the 1.8−7 K temperature range. Diamagnetic corrections were estimated from Pascal tables. The fit was performed minimizing the function $R = \Sigma(\chi_M T_{exp} - \chi_M T_{cal})^2/\Sigma(\chi_M T_{exp})^2$. The $\chi_M T$ vs T curves at 500 and 10 000 G overlay.

EPR spectra of crushed small crystals of **1**·8H_2O were recorded at the X-band (9.4 GHz) frequency with a Bruker ESP-300E spectrometer, at room temperature and 5 K, at the Servei de Magnetoquímica of the Universitat de Barcelona.

EPR Simulation. A program written by H. Weihe[29] was used to simulate powder EPR spectra. The simulation was performed by generating the energy matrix for each orientation of the molecule relative to the magnetic field. The resonance condition for each transition was then found by successive diagonalizations and iterations of the energy matrix, and the relative intensities were calculated from the eigenvectors multiplied by the appropriate Boltzmann factor at 5 K. Summation of all the transitions over the whole space, where each transition is represented by a differentiated Gaussian curve, gives the simulated spectrum. The spin Hamiltonian used for the simulation include the ZFS parameters D and E.

Computational Details. A detailed description of the computational strategy to calculate the exchange coupling constants in polynuclear complexes is outside the scope of this paper. In this work, we have followed a procedure extensively described in previous papers.[30−32] The exchange coupling constants are introduced by a phenomenological Heisenberg Hamiltonian $H = -\Sigma J_i S_j S_k$ (where i labels the different kind of exchange constants, and j and k make reference to the different paramagnetic centers) to describe the interactions between each pair of paramagnetic transition metals present in the polynuclear complex. For all practical purposes, to evaluate the different nJ_i coupling constants in one complex, we need to perform at least the calculations for $n + 1$ different spin distributions and to solve the n equations system obtained from the energy differences between diagonal terms of the Hamiltonian matrix. Thus, for instance, the equation corresponding to the energy difference between the high-spin distribution (all of the paramagnetic centers with spin up) and the spin distribution (LS1) with Cu1 and Cu3 cations with spin down (see Scheme 2) can be easily obtained, as it is described in ref 31, by analyzing the changes of the sign of the interactions. There are changes in the J_1, J_2, and J_4 interactions between both spin distributions (see Scheme 2) resulting in the following equation

$$E_{HS} - E_{LS1} = -J_1 - J_2 - 2J_4 \quad (1)$$

Hydrogen atoms were included in the dangling bonds of the dinuclear models employed to check the countercomplementarity effect to preserve the neutral charge of the molecule, avoiding negative values.

The hybrid B3LYP functional[33] has been used in all of the calculations as implemented in Gaussian-98[34] by mixing the exact Hartree−Fock-type exchange with Becke's expression for the exchange functional[35] and that proposed by Lee−Yang−Parr for the correlation contribution.[36] Such a functional provides calculated J values in excellent agreement with the experimental values.[30,37,38] Basis sets proposed by Schaefer et al. have been employed throughout, with triple-ζ quality for the copper atoms[39] and double-ζ for the main group elements.[40]

Results and Discussion

$[(Cu_2L)_2(CO_3)]$·8H_2O (**1**·8H_2O) was obtained by two different synthetic routes, a chemical method and electrochemical synthesis. The chemical method consists of the reaction of $Cu_2L(OAc)$·6H_2O[26a] with NMe_4OH·5H_2O in methanol or acetonitrile in air. This indicates that the acetate complex can act as a carbon dioxide scrubber in a basic medium, to convert it into carbonate. Such a reaction is not without precedent, as it is well-known that basic solutions of transition metal complexes can react with CO_2 from air. However, this reaction usually yields dinuclear and trinuclear copper complexes, and higher nuclearities are still far less common. In fact, systematic methods to isolate tetranuclear carbonate compounds are scarcely described in the litera-

(27) *SADABS, Area-Detector Absorption Correction*; Siemens Industrial Automation Inc.: Madison, WI, 1996.
(28) Sheldrick, G. M. *SHELX97 Programs for Crystal Structure Analysis*; Institüt für Anorganische Chemie der Universität: Göttingen, Germany, 1998.
(29) The simulation software package is freely distributed by Dr. H. Weihe; for more information see the www page: http://sophus.kiku.dk/software/EPR/EPR.html
(30) Ruiz, E.; Alemany, P.; Alvarez, S.; Cano, J. *J. Am. Chem. Soc.* **1997**, *119*, 1297.
(31) Ruiz, E.; Rodríguez-Fortea, A.; Cano, J.; Alvarez, S.; Alemany, P. *J. Comput. Chem.* **2003**, *24*, 982.
(32) Ruiz, E.; Cano, J.; Alvarez, S.; Alemany, P. *J. Comput. Chem.* **1999**, *20*, 1391.
(33) Becke, A. D. *J. Chem. Phys.* **1993**, *98*, 5648.
(34) Frisch, M. J.; Trucks, G. W.; Schlegel, H. B.; Scuseria, G. E.; Robb, M. A.; Cheeseman, J. R.; Zakrzewski, V. G.; Montgomery, J. A.; Stratmann, R. E.; Burant, J. C.; Dapprich, S.; Millam, J. M.; Daniels, A. D.; Kudin, K. N.; Strain, M. C.; Farkas, O.; Tomasi, J.; Barone, V.; Cossi, M.; Cammi, R.; Mennucci, B.; Pomelli, C.; Adamo, C.; Clifford, S.; Ochterski, J.; Petersson, G. A.; Ayala, P. Y.; Cui, Q.; Morokuma, K.; Malick, D. K.; Rabuck, A. D.; Raghavachari, K.; Foresman, J. B.; Cioslowski, J.; Ortiz, J. V.; Stefanov, B. B.; Liu, G.; Liashenko, A.; Piskorz, P.; Komaromi, I.; Gomperts, R.; Martin, R. L.; Fox, D. J.; Keith, T.; Al-Laham, M. A.; Peng, C. Y.; Nanayakkara, A.; Gonzalez, C.; Challacombe, M.; Gill, P. M. W.; Johnson, B. G.; Chen, W.; Wong, M. W.; Andres, J. L.; Head-Gordon, M.; Replogle, E. S.; Pople, J. A. *Gaussian 98*, Revision A.11; Gaussian Inc.: Pittsburgh, PA, 1998.
(35) Becke, A. D. *Phys. Rev. A* **1988**, *38*, 3098.
(36) Lee, C.; Yang, W.; Parr, R. G. *Phys. Rev. B* **1988**, *37*, 785.
(37) Ruiz, E.; Cano, J.; Alvarez, S.; Alemany, P. *J. Am. Chem. Soc.* **1998**, *120*, 11122.
(38) Ruiz, E.; Alvarez, S.; Rodríguez-Fortea, A.; Alemany, P.; Pouillon, Y.; Massobrio, C. In *Electronic Structure and Magnetic Behavior in Polynuclear Transition-metal Compounds*; Miller, J. S., Drillon, M., Weinheim, M., Eds.; Wiley-VCH: Weinheim, Germany, 2001.
(39) Schaefer, A.; Huber, C.; Ahlrichs, R. *J. Chem. Phys.* **1994**, *100*, 5829.
(40) Schaefer, A.; Horn, H.; Ahlrichs, R. *J. Chem. Phys.* **1992**, *97*, 2571.

ture,[12,17] and the nuclearity of the complex seems to depend to a great extend on the copper salt employed[12] and on the reaction conditions (the quantity of water present in the reaction medium, time of exposure to air, etc).[17] In our case study, these conditions do not seem to play as important of a role as the complex can be isolated by two such disparate routes as the previously mentioned chemical method and in an electrochemical cell. Furthermore, in both cases the complex is unique, and the reaction proceeds in a short time period. In addition, we have recently published that a similar tetranuclear zinc complex could also be isolated by means of these two synthetic procedures.[41] Therefore, it seems that the type of ligand employed in this work favors the tetranuclearity and that the described routes appear to constitute easy ways of obtaining tetranuclear carbonate complexes from metal precursors and adventitious carbon dioxide.

Spectroscopic, spectrometric, and analytical methods were of some use in the structural elucidation of the present complex, but X-ray crystallographic determinations were required to show the full details. Thus, the IR spectrum of **1**·8H_2O contains a sharp band at 1633 cm^{-1}, in agreement with the coordination of the Schiff base to the metal atoms through the imine nitrogen atoms. Two sharp absorption bands at 1535 and 1342 cm^{-1} are consistent with the presence of the carbonate ligand,[41−43] and a wide band centered at 3425 cm^{-1} agrees with the hydration of the complex. The electrospray ionization (ESI) mass spectrum shows the existence of dinuclear units in solution, with a peak at ca. 581 (100%) *m*/*z*, corresponding to $[Cu_2L]^+$ fragments. However, peaks related to the whole carbonate complex could not be assigned. This is may be because of the neutral nature of the tetranuclear molecule.

Crystal Structure of {[(Cu$_2$L)$_2$(CO$_3$)]}$_2$·12H$_2$O (1·6H$_2$O). Crystals of **1**·6H_2O were obtained as detailed above. An ORTEP view of **1** is shown in Figure 1. Experimental details are given in Table 1 and selected bond lengths and angles in Table 2.

The asymmetric unit of **1**·6H_2O contains two crystallographically different $[(Cu_2L)_2(CO_3)]$ molecules that will be called **1a** and **1b**. Additionally, 16 water molecules are present in the unit cell, with 6 of them at partial occupancies, adding up a total of 12 water solvates.

1a and **1b** are quite similar, despite significant geometric differences and will be discussed together. Both molecules can be understood as self-assembled from two dinuclear $[Cu_2L]^+$ units bridged by the carbonate ligand (Figure 2), giving rise to tetranuclear copper entities. The labels of the atoms are in agreement with this consideration. Thus, the first number of the labels indicates the dinuclear moiety under discussion ($X = 1, 2$ for the $[Cu_2L]^+$ units of **1a** and $X = 3, 4$ for the $[Cu_2L]^+$ units of **1b**).

The four copper atoms are placed on the vertexes of a distorted rectangle, with the carbonate ligand lying in the center of the rectangle and showing a μ_4-η^2:η^1:η^1 coordination mode: one oxygen atom bridges both metal centers of the same $[Cu_2L]^+$ unit and the remaining two oxygen atoms are linked in a syn−syn binding mode to each one of the copper ions of the second dinuclear cation. It is remarkable that this is the first copper complex of this type where the carbonate ligand is not disordered.

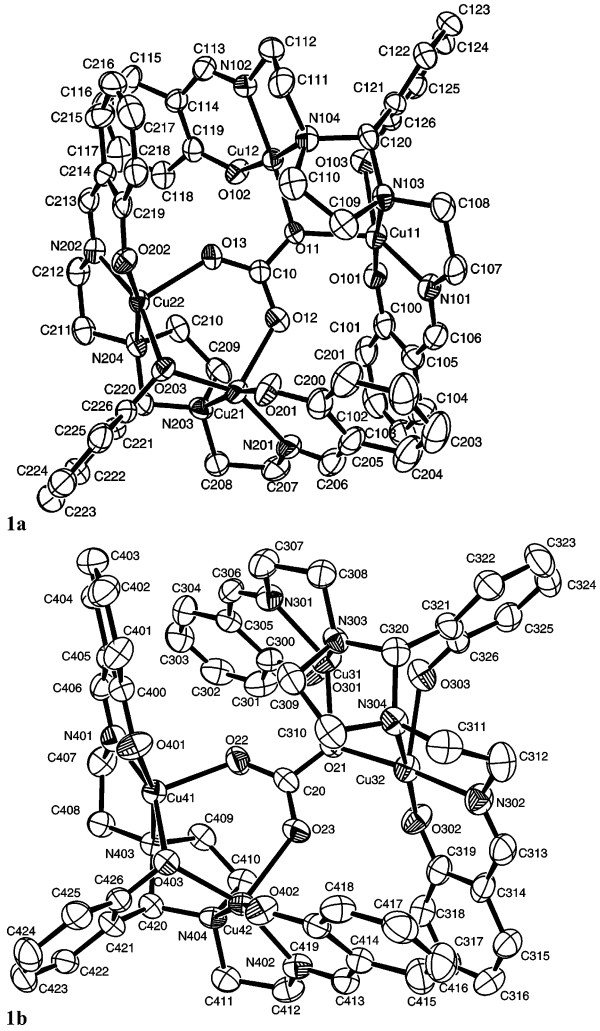

Figure 1. An ORTEP view of the crystal structure of **1**. Ellipsoids are drawn at 40% probability.

The $[Cu_2L]^+$ fragments show that the ligand $[L]^{3-}$ provides two N_2O compartments, every one allocating a copper atom. In addition, the central ligand arm affords a phenoxo oxygen donor, which shows different coordination behavior for each ligand of the same tetranuclear molecule:

(1) For one $[Cu_2L]^+$ fragment ($X = 2$ for **1a**, 4 for **1b**), the phenoxo oxygen atom of the middle ligand arm [O(X03)] joins both metal centers. This gives rise to a quite symmetric $Cu-O_{phenoxo}-Cu$ bridge, as reflected by the Cu−O(X03) distances. Therefore, the two copper atoms of this unit show two different bridges: $Cu-O,O_{carbonate}-Cu$, and $Cu-O_{phenoxo}-Cu$, with distances Cu(X1)···Cu(X2) of ca. 3.3 Å. The $Cu-O_{phenoxo}-Cu$ angles are 110.2(3)° and 114.8(3)° for **1a** and **1b**, respectively, with the Cu−O−Cu ideal plane nearly perpendicular to the central aromatic ring (89.19° for **1a** and 90.64° for **1b**).

(41) Fondo, M.; García-Deibe, A. M.; Bermejo, M. R.; Sanmartín, J.; Llamas-Saiz, A. L. *J. Chem. Soc., Dalton Trans.* **2002**, 4746.
(42) Bauer-Siebenlist, B.; Meyer, F.; Vidovic, D.; Pritzkow, H. *Z. Anorg. Allg. Chem.* **2003**, *629*, 2152.
(43) Doyle, R. P.; Kruger, P. E.; Moubaraki, B.; Murray, K. S.; Nieuwenhuyzen, M. *J. Chem. Soc., Dalton Trans.* **2003**, 4230.

Table 2. Main Distances (Å) and Angles (deg) for **1**·6H_2O

1a		1b		1a		1b	
Cu(11)−O(101)	1.937(6)	Cu(32)−O(302)	1.925(6)	Cu(12)···Cu(22)	4.889(2)	Cu(32)···Cu(42)	4.837(2)
Cu(11)−N(101)	1.965(7)	Cu(32)−N(302)	1.949(7)	O(101)−Cu(11)−O(11)	93.5(2)	O(302)−Cu(32)−O(21)	92.8(3)
Cu(11)−O(11)	2.055(5)	Cu(32)−O(21)	2.003(6)	N(101)−Cu(11)−O(11)	131.8(3)	N(302)−Cu(32)−O(21)	138.8(3)
Cu(11)−N(103)	2.075(7)	Cu(32)−N(304)	2.085(7)	O(101)−Cu(11)−N(103)	173.6(3)	O(302)−Cu(32)−N(304)	174.7(3)
Cu(11)−O(103)	2.093(6)	Cu(32)−O(303)	2.225(6)	O(11)−Cu(11)−N(103)	90.6(2)	O(21)−Cu(32)−N(304)	91.4(3)
Cu(12)−O(102)	1.898(5)	Cu(31)−O(301)	1.902(5)	N(101)−Cu(11)−O(103)	146.6(3)	N(302)−Cu(32)−O(303)	141.9(3)
Cu(12)−N(102)	1.932(6)	Cu(31)−N(301)	1.921(8)	O(11)−Cu(11)−O(103)	80.5(2)	O(21)−Cu(32)−O(303)	78.0(2)
Cu(12)−O(11)	1.935(7)	Cu(31)−O(21)	1.941(6)	O(11)−Cu(12)−N(102)	171.9(3)	N(301)−Cu(31)−O(21)	170.9(3)
Cu(12)−N(104)	2.135(7)	Cu(31)−N(303)	2.146(7)	O(102)−Cu(12)−N(104)	173.4(3)	O(301)−Cu(31)−N(303)	170.8(3)
Cu(12)···O(103)	2.467(7)	Cu(31)···O(303)	2.404(7)	N(201)−Cu(21)−O(203)	152.4(3)	N(401)−Cu(41)−O(403)	161.4(3)
Cu(21)−O(201)	1.925(7)	Cu(41)−O(401)	1.949(6)	O(201)−Cu(21)−N(203)	169.6(3)	O(401)−Cu(41)−N(403)	165.8(3)
Cu(21)−N(201)	1.963(7)	Cu(41)−N(401)	1.948(7)	O(201)−Cu(21)−O(12)	93.2(3)	O(401)−Cu(41)−O(22)	93.9(3)
Cu(21)−O(203)	1.990(6)	Cu(41)−O(403)	1.957(5)	N(201)−Cu(21)−O(12)	99.4(3)	N(401)−Cu(41)−O(22)	98.9(3)
Cu(21)−N(203)	2.117(8)	Cu(41)−N(403)	2.126(7)	O(203)−Cu(21)−O(12)	107.9(2)	O(403)−Cu(41)−O(22)	99.4(2)
Cu(21)−O(12)	2.129(6)	Cu(41)−O(22)	2.094(6)	N(203)−Cu(21)−O(12)	96.7(3)	N(403)−Cu(41)−O(22)	99.9(3)
Cu(22)−O(202)	1.942(5)	Cu(42)−O(402)	1.938(6)	N(202)−Cu(22)−O(203)	161.2(3)	N(402)−Cu(42)−O(403)	158.2(3)
Cu(22)−N(202)	1.960(7)	Cu(42)−N(402)	1.960(7)	O(202)−Cu(22)−N(204)	167.4(3)	O(402)−Cu(42)−N(404)	166.1(3)
Cu(22)−O(203)	1.978(5)	Cu(42)−O(403)	1.966(5)	O(202)−Cu(22)−O(13)	89.6(2)	O(402)−Cu(42)−O(23)	98.4(3)
Cu(22)−N(204)	2.081(7)	Cu(42)−N(404)	2.115(7)	N(202)−Cu(22)−O(13)	95.8(3)	N(402)−Cu(42)−O(23)	97.8(3)
Cu(22)−O(13)	2.119(6)	Cu(42)−O(23)	2.089(6)	O(203)−Cu(22)−O(13)	102.8(2)	O(403)−Cu(42)−O(23)	103.8(2)
Cu(11)···Cu(12)	3.2201(17)	Cu(31)···Cu(32)	3.2305(18)	N(204)−Cu(22)−O(13)	102.0(3)	N(404)−Cu(42)−O(23)	95.3(3)
Cu(21)···Cu(22)	3.2543(17)	Cu(41)···Cu(42)	3.3043(17)	Cu(22)−O(203)−Cu(21)	110.2(3)	Cu(41)−O(403)−Cu(42)	114.8(3)
Cu(11)···Cu(21)	5.254(2)	Cu(31)···Cu(41)	5.030(2)	Cu(12)−O(11)−Cu(11)	109.0(2)	Cu(31)−O(21)−Cu(32)	111.6(3)

Accordingly, the metal atoms of this unit are in an N_2O_3 environment, with the coordination sphere made up of the N_2O donor set of one cavity of the ligand, one oxygen atom of the bidentate carbonate linkage (O(X2) or O(X3)), and the central phenoxo oxygen atom O(X03). Analysis of the τ parameter (0.287, 0.103, 0073, and 0.130 for Cu(21), Cu(22), Cu(41), and Cu(42), respectively) indicates a distorted square pyramidal geometry for the copper atoms. Both pyramids of the same $[Cu_2L]^+$ moiety share O(X03) as a basal vertex, with the carbonate oxygen atom (O(X2) or O(X3)) at the apex. It is remarkable that, to the best of our knowledge, this is the first μ_4-η^2:η^1:η^1 carbonate copper complex where the μ_2-O,O atoms occupy apical sites of the polyhedron. The calculated mean basal planes of the pyramids form angles of 38.81(25)° and 34.39(26)° for **1a** and **1b**, respectively, showing the non-coplanarity induced by the constrained ligand.

(2) For the second $[Cu_2L]^+$ moiety (X = 1, 3) of the tetranuclear complex, the phenoxo oxygen atom of the central arm, O(X03), is just coordinated to one metal center, Cu(11) in **1a** and Cu(32) in **1b**. The distance of this oxygen atom to the second metal center is quite long to be considered as a true coordination bond and should be best described as a secondary intramolecular interaction. Therefore, both copper ions are single bridged by the carbonate oxygen atom O(X1), with Cu(X1)···Cu(X2) distances of ca. 3.2 Å. The Cu−O(X1) bond lengths reflect the asymmetry of this bridge, with a Cu−O(X1)−Cu angle of ca. 110°. This situation gives rise to one copper atom in an N_2O_2 environment (Cu(12) in **1a** and Cu(31) in **1b**) and one in an N_2O_3 environment (Cu(11) in **1a** and Cu(32) in **1b**). The geometry around Cu(12) and Cu(31) is distorted square planar, with Cu(12) above (+0.1427(37) Å) and Cu(31) below (−0.0933(32) Å) the mean-square-calculated plane.

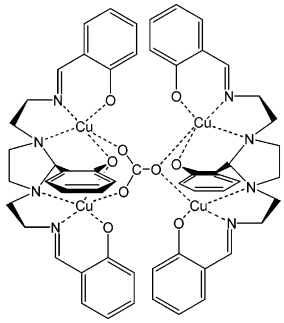

Figure 2. Schematic representation of the $[(Cu_2L)_2(CO_3)]$ complex.

The geometry of the N_2O_3 pentacoordinated centers is highly distorted, as the τ parameter reflects (0.45 for Cu(11) and 0.55 for Cu(32)). A strict reading of these values seems to indicate that the geometry for Cu(11) (**1a**) is closer to the square pyramid and for Cu(32) (**1b**) to the trigonal bipyramid. However, an analysis of the bond lengths and angles shows that these parameters do not reasonably match with any of the geometries and that the situation should be best considered as intermediate.

As a result of all the discussed geometrical features, **1a** and **1b** present the unfamiliar characteristic of various coordination polyhedra for the four copper atoms: square pyramid (Cu(21) and Cu(22) in **1a** and Cu(41) and Cu(42) in **1b**), square planar (Cu(12) in **1a** and Cu(31) in **1b**), and intermediate between square pyramid and trigonal bipyramid (Cu(11) in **1a** and Cu(32) in **1b**).

Finally, it is worth noting that the copper atoms of the same $[Cu_2L]^+$ fragment are bridged by a NCN function [N(X03)C(X20)N(X04)], in addition to the carbonate and phenoxo linkages described, and this is a common structural singularity for all of the $[Cu_2L]^+$ dinuclear cations.

The X-ray powder diffractogram of **1**·8H_2O has been recorded and compared with the one of **1**·6H_2O, simulated from experimental single X-ray data. Both diffractograms are quite similar, indicating that the number of water solvates present in the unit cell does not seem to significantly affect the structure of the tetranuclear complex.

Magnetic Measurements. The magnetic properties of **1**·8H_2O have been investigated in the 2−300 K temperature

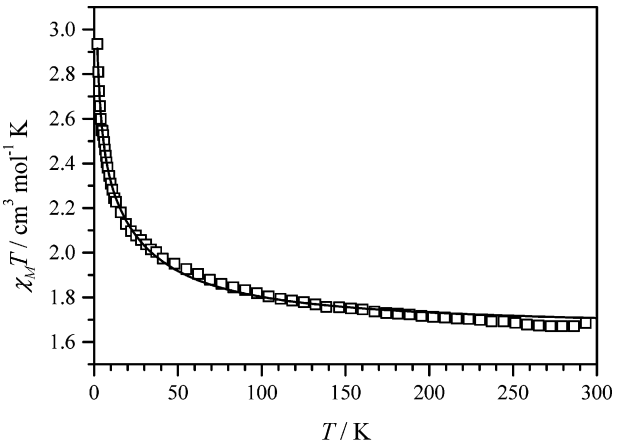

Figure 3. $\chi_M T$ vs T plot: squares, experimental data and solid line, fit with $J_1 = 12.42$ cm^{-1}, $J_2 = 39.44$ cm^{-1}, $J_3 = 0.5$ cm^{-1}, $J_4 = -1.26$ cm^{-1}, and $g = 2.1$.

range. The $\chi_M T$ value at room temperature is 1.67 cm^3 mol^{-1} K, which is the expected one for the four Cu(II) ions with a g value of 2.11. The $\chi_M T$ product increases with decreasing temperature, reaching a maximum of 2.93 cm^3 mol^{-1} K at 2 K (Figure 3). This behavior is characteristic of ferromagnetic coupling, although the observed $\chi_M T$ maximum value is lower than the ordinary one for a ground state of $S = 2$ (3.39 cm^3 mol^{-1} K with $g = 2.11$).

Magnetization measurements at 2 K follow Brillouin's law predictably for an $S = 2$ state, in agreement with the ferromagnetic behavior observed. Besides, magnetization measurements were recorded in the temperature range of 1.8−7 K at different magnetic fields from 2500 to 30 000 G. The obtained $M/N\beta$ vs H/T graphs superimpose (Figure S1), indicating small zero field splitting.

Several models were tested to explain the magnetic behavior, on the basis of the structural data obtained by single X-ray diffraction studies. In a first approach, **1** can be considered as two dinuclear complexes composed of (a) Cu(1)···Cu(2), bridged by one oxygen atom of the CO_3^{2-} ligand in a μ_2-η^2-O fashion and (b) Cu(3)···Cu(4), bridged by one phenoxo group and by the carbonate ligand in a μ_2-η^1:η^1-O,O mode (see Scheme 2).

The experimental $\chi_M T$ values do not fit well with this approach of two dinuclear sites with J_1 for Cu(1)···Cu(2) and J_2 for Cu(3)···Cu(4). Therefore, the interactions through the carbonate ligand coordinated in a syn−anti fashion (Cu(1)···Cu(3) and Cu (2)···Cu(4) with J_3) and the crossed interactions (Cu(2)···Cu(3) and Cu(1)···Cu(4), with J_4) were considered. The spin Hamiltonian used for the fitting with the CLUMAG program[44] was $H = -J_1(S_1 \cdot S_2) - J_2(S_3 \cdot S_4) - J_3(S_1 \cdot S_3 + S_2 \cdot S_4) - J_4(S_1 \cdot S_4 + S_2 \cdot S_3)$.

Different sets of parameters can be obtained; in all cases, the g value is close to 2.1 and J_1 and J_2 are ferromagnetic and more important than J_3 and J_4, as expected. The best fit gave values of $J_1 = 12.42$ cm^{-1}, $J_2 = 39.44$ cm^{-1}, $J_3 = 0.50$ cm^{-1}, $J_4 = -1.26$ cm^{-1}, and $g = 2.1$ ($R = 9.3 \times 10^{-5}$) (Figure 3), but other sets of parameters also fit well with the experimental values, as $J_1 = 16.31$ cm^{-1}, $J_2 = 30.00$ cm^{-1}, $J_3 = -0.50$ cm^{-1}, $J_4 = 2.24$ cm^{-1}, and $g = 2.1$ ($R = 1.2 \times 10^{-4}$).

Scheme 2

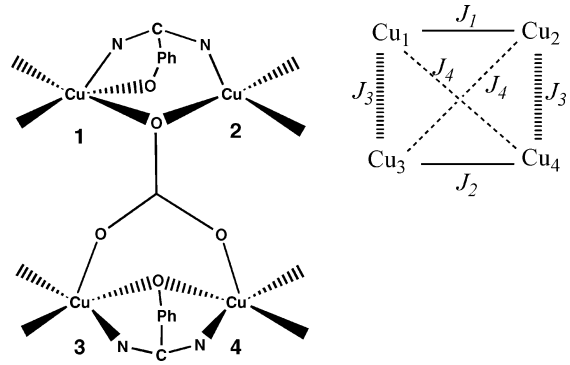

From these results, it can be clearly inferred: (a) that the two dinuclear sites (Cu(1)···Cu(2) and Cu(3)···Cu(4)) show the major ferromagnetic contribution, but it is not possible to assign J_1 and J_2 to an specific site, and (b) that the interactions through the syn−anti carbonate ligand are weak and, at least, one of them can be antiferromagnetic.

As discussed before, Cu(1) and Cu(2), bridged by one oxygen atom of the carbonate ligand, show different coordination polyhedra: one copper ion is in a square planar environment while the geometry for the other one is an intermediate between square pyramid and trigonal bipyramid. Therefore, the bridging oxygen atom can be considered as swinging between a basal−apical and basal−basal position of the idealized coordination polyhedra (Figure 4). Cu(3) and Cu(4) are bridged by the carbonate ligand in a syn−syn fashion, and these oxygen atoms are the apical vertexes of the square pyramids. Besides, Cu(3) and Cu(4) also share a phenol oxygen atom as a basal vertex of their square pyramidal chromophores. Thus, to understand the factors that govern the magnetic behavior of **1**, compounds with close structural features were revised.

Different carbonate complexes with a similar coordination mode of the carbonate ligand to that found in **1** are listed in Table 3. The magnetic interaction through the μ_2-η^2-O atom of the carbonate bridge can be ferro- or antiferromagnetic. On one hand, this interaction seems to be weak and ferromagnetic when the oxygen atom occupies a basal vertex of one polyhedron and the apical position of the other one, as in $[Cu_6(bpy)_{10}(\mu\text{-}CO_3)_2(\mu\text{-}OH)_2](ClO_4)_6$.[18] On the other hand, strong antiferromagnetism is observed when the

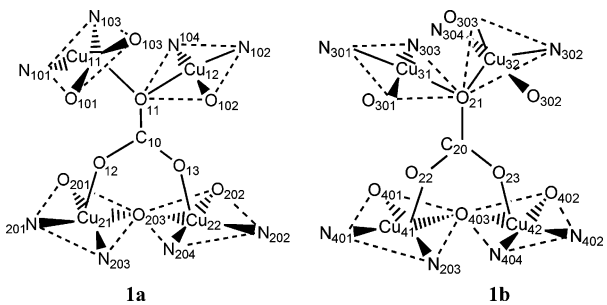

Figure 4. Schematic representation of the core of **1a** and **1b**, depicting the two extreme geometric situations around the copper atoms.

(44) Gatteschi, D.; Pardi, L. CLUMAG Program. *Gazz. Chim. Ital.* **1993**, *123*, 231.

Table 3. Carbonate Complexes with Similar Coordination Mode to Compound **1**. The J Values Correspond to the Spin Hamiltonian $H = -J\,S_1 \cdot S_2$

compound	J (cm^{-1})	#	α (°)	ref
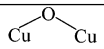				
$[Cu_6(bpy)_{10}(\mu\text{-}CO_3)_2(\mu\text{-}OH)_2](ClO_4)_6$ [a]	3.25	b–a	124	18
$[Cu_4(bapa)_4(\mu_4\text{-}CO_3)(\mu\text{-}Br)_2]Br_4$ [b]	- 275	b–b	128.4	12
$[Cu_4(bapma)_4(\mu_4\text{-}CO_3)(\mu\text{-}Cl)_2]Cl_4$ [c]	- 390	b–b	129.3	12
$[Cu_4(dpt)_4(\mu_4\text{-}CO_3)(\mu\text{-}Cl)_2](ClO_4)_4$ [d]	- 190	b–b	121	17
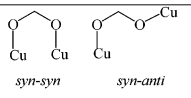 *syn-syn* *syn-anti*				
$[Cu_6(bpy)_{10}(\mu\text{-}CO_3)_2(\mu\text{-}OH)_2](ClO_4)_6$ [a]	2.75	b–b	*syn-anti*	18
$[Cu(CO_3)(4\text{-apy})_2]_n$ [e]	11	b–b	*syn-anti*	15
$[Cu_2(ascidH_2)(\mu\text{-}CO_3(H_2O)_2]$ [f]	1.6	b–b	*syn-anti*	19
$[Cu_4(bapa)_4(\mu_4\text{-}CO_3)(\mu\text{-}Br)_2]Br_4$ [b]	- 31	b–b	*syn-syn*	12
$[Cu_4(bapma)_4(\mu_4\text{-}CO_3)(\mu\text{-}Cl)_2]Cl_4$ [c]	-26	b–b	*syn-syn*	12
$[Cu_4(dpt)_4(\mu_4\text{-}CO_3)(\mu\text{-}Cl)_2](ClO_4)_4$ [d]	- 22	b–b	*syn-syn*	17

[#] Position occupied by the oxygen atom in the coordination polyhedra of the Cu(II) ions, b = basal and a = apical. [a] bpy = 2,2′-bipirydine. [b] bapa = bis(3-aminopropyl)amine. [c] bapma = bis(3-aminopropyl)methylamine. [d] dpt = bis(3-aminopropyl)amine. [e] 4-apy = 4-aminopyridine. [f] $ascidH_2$ = ascidiacyclamide.

oxygen atom is shared by the basal planes of the square pyramids, as reported for the other tetranuclear complexes described in the literature.[12,17] In compound **1**, a small antiferromagnetic interaction should be expected due to the particular location of the μ_2-η^2-O atom of the carbonate ligand (basal−apical and basal−basal) and the degree of distortions.

When the carbonate ligand bridges both Cu(II) ions in a μ_2-η^1:η^1-O,O mode, with the oxygen atoms placed in basal positions, the magnitude of the magnetic interaction is usually small, and it can be ferro- or antiferromagnetic. In compound **1**, these oxygen atoms occupy the apical positions of the polyhedra, and this way of interaction can be considered irrelevant.

Moreover, the number of copper(II) compounds with only one phenoxo bridging ligand described in the literature is limited. Table 4 summarizes the complexes with a square pyramidal arrangement around the Cu(II) ions and only one phenoxo bridging ligand. This kind of complex shows weak ferromagnetic (or negligible) interaction when the oxygen atom of the phenoxo group is in basal−apical or apical−apical positions.[20−22,25] In contrast, when the oxygen atom is shared by the basal plane of both coordination polyhedra, a strong antiferromagnetic interaction is operative.[23,24] The magnetic properties of $[Cu_2L(AcO)]$[26a] constitute the only exception to this behavior. In this case, despite the basal−basal location of the phenol oxygen atom, a net ferromagnetic

Table 4. Magnetic Interaction for Cu(II) Complexes with Only One Phenoxo Bridging Ligand ($H = -J\,S_1 \cdot S_2$)

	J (cm^{-1})	#[a]	ref
$(Cu_2L(H_2O)_2)(ClO_4)_3$[b]	4.2	b−a	20
$(Cu_2(L^1)Cl_2)ClO_4$[c]	0	a−a	21
$(Cu_2(CH_3HXTA)(H_2O)_2)H$[d]	0	b−a	22
$Na(Cu_2(CH_3HXTA)(py)_2)$[d]	−168	b−b	23
$(Cu_2L(NO_2)_2(H_2O)_2)ClO_4$[e]	−122	b−b	24
$(Cu_4L(OH)_2)(CF_3SO_3)_2$[f]	0	a−a	25
$(Cu_2L(AcO))$[g]	49.2[h]	b−b	26a

[a] # respresents the position occupied by the oxygen atom in the coordination polyhedra of the Cu(II) ions, b = basal and a = apical. [b] L = anion of 2,6-bis[(bis(benzimidazolylmethyl)amino)methyl]-*p*-cresol. [c] HL^1 = 2,6-bis[bis(2-pyridylmethyl)-aminomethyl]-4-methylphenol. [d] CH3HXTA = *N*,*N*′-(2-hydroxy-5-methyl-1,3-xylylene)bis(*N*-carboxymethylglycine).[e] LH = 2,6-bis(*N*-methylpiperazino)methyl)-4-chlorophenol. [f] L = octaaminotetraphenol. [g] H_3L = 2-(2-hydroxyphenyl)-1,3-bis[4-(2-hydroxyphenyl)-3-azabut-3-enyl]-1,3-imidazolidine. [h] This compound shows one acetate bridge in apical positions also, and L is the same ligand as in compound **1**.

coupling was observed. $[Cu_2L(MeO)]$,[26b] containing a phenoxo bridging moiety as the common apical vertex and a methanolate bridging ligand as a common basal position, shows the same magnetic pattern, and in this case, the ferromagnetic coupling seems to be mainly mediated by the methanolate oxygen atom. Compound **1**, with the same heptadentate Schiff base ligand, also shows a global ferromagnetic interaction.

Therefore, comparison with the literature does not help to elucidate the origin of the described magnetic behavior. Consequently, DFT calculations with the experimental atomic coordinates of **1** were performed to obtain the J values for such system and to try to assign the different coupling constants. As previously indicated, complex **1** has two crystallographically different molecules in the unit cell. Accordingly, we have calculated the J values for both molecules (see Scheme 2), with the following results: **1a,** $J_1 = 11.0$ cm^{-1}, $J_2 = 25.8$ cm^{-1}, $J_3 = 0.11$ cm^{-1}, and $J_4 = 1.3$ cm^{-1}; **1b**, $J_1 = 11.1$ cm^{-1}, $J_2 = 21.5$ cm^{-1}, $J_3 = -0.06$ cm^{-1}, and $J_4 = 2.1$ cm^{-1}. The calculated J values are very similar in both cases and reproduce the trends of the CLUMAG fitting: (a) J_1 and J_2 are the strongest coupling constants and both are ferromagnetic, with J_2 being larger than J_1 (see Scheme 2); (b) the magnetic coupling through the carbonato ligand (J_3 and J_4) is very weak. The J_4 coupling constant is ferromagnetic, while the J_3 coupling constant is very small and to predict the sign of this interaction is beyond the accuracy of the employed method.

The two sets of DFT calculated J values (one for each crystallographic molecule) were used in the CLUMAG program[44] to create the theoretical $\chi_M T$ *vs* T plot for both complexes (**1a** and **1b**). The curves with the estimated J values (see Figure 5) are in good agreement with the experimental data. The shape of the graph between 50 and 100 K is very sensitive to J_2, and the calculated curve shows its maximum deviation from the experimental one in this area. A larger calculated J_2 value would give a better match of both curves in this region. In fact, the best fit of the experimental data is obtained with $J_2 \sim 30-40$ cm^{-1}, as indicated above.

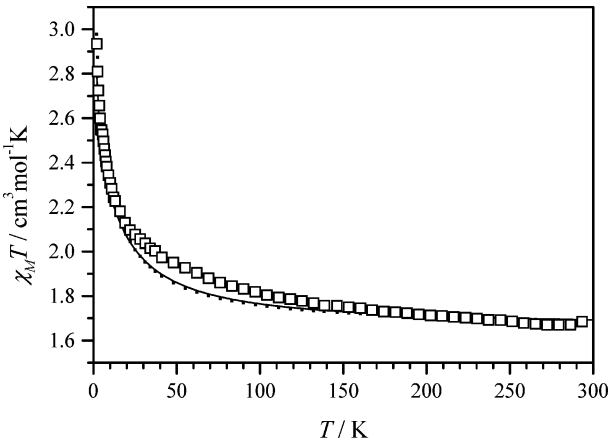

Figure 5. Graph of the $\chi_M T$ vs T plot, simulated with the exchange coupling constants calculated with the B3LYP functional. The two nearly superimposed lines correspond to the simulated graph with the parameters obtained for complexes **1a** and **1b** (solid and dashed line, respectively). The squares are the experimental data to allow comparison. The g value was fixed at $g = 2.1$.

The DFT calculations also allow assigning J_1 and J_2 to a specific site. Thus, the strongest interaction (J_2) occurs between Cu(3) and Cu(4), which seems to be mediated by the μ_2-η^2-O_{phenol} atom, while the μ_2-η^2-$O_{carbonate}$ bridge seems to promote a weaker ferromagnetic coupling between Cu(1) and Cu(2) (J_1).

Therefore, the DFT calculations are in good agreement with experimental results and allow assigning each coupling constant to and specific site. However, the origin of the relatively large J_1 and J_2 positive values is still unclear since the bridging ligands involved in such exchange pathways usually favor antiferromagnetism (see Tables 3 and 4).[17,45] Consequently, the structure of the complex was once again analyzed, and this more accurate analysis shows the presence of an additional NCN bridge, supplied by the Schiff base ligand. Thus, the J_1 coupling constant includes the sum of two contributions: a single-oxygen bridging atom from the carbonato ligand and an NCN bridge from the Schiff base. In the same way, the J_2 coupling constant is made of three different contributions: a μ_2-η^1:η^1-O,O carbonato ligand, a bridging phenoxo oxygen atom, and an NCN bridge from the Schiff base ligand.

New DFT calculations were performed on models including all of the mentioned bridging ligands to clarify the origin of the ferromagnetism. Accordingly, each tetranuclear molecule (**1a** and **1b**) was modeled as two dinuclear entities: Cu(1)···Cu(2) (with J_1 interaction) and Cu(3)···Cu(4) (with J_2 interaction), and the magnetic coupling constants of the dinuclear models were calculated. Computations were performed with the whole dinuclear model and eliminating the bridging ligands one by one.

The J_1 and J_2 values obtained from the calculations with the whole model molecules are comparable to those found with the experimental atomic coordinates of the tetranuclear complex (see Table 5). Elimination of the NCN bridge between Cu(1)···Cu(2) shows an antiferromagnetic contribution of the carbonate ligand. For the model containing Cu(3)···Cu(4), removal of the carbonate ligand, which fills axial coordination sites, shows a small change in the J values.

Table 5. Exchange Coupling Constants and Energy Gap of SOMOs Corresponding to the Triplet State Calculated with the B3LYP Functional for Different Dinuclear Models for the J_1 and J_2 Interactions of the Two Complexes **1a** and **1b** Reducing the Number of Active Bridging Ligands

	1a		**1b**	
bridging ligands	J (cm^{-1})	ΔE (au)	J (cm^{-1})	ΔE (au)
	exchange pathway J_1			
O (CO_3^{2-}), NCN	+8.8 (+11.0)[a]	0.003	+7.7 (+11.1)	0.005
O (CO_3^{2-})	−26.8	0.016	−38.7	0.018
	exchange pathway J_2			
OCO, NCN, O (OPh)	+23.3 (+25.8)	0.011	+18.0 (+21.5)	0.010
NCN, O (OPh)	+26.6	0.012	+15.5	0.015
O (OPh)	−29.7	0.016	−50.8	0.018

[a] Values in parentheses correspond to the calculated J values using the whole structure of the complexes.

However, when the NCN link is eliminated, the resulting coupling through the phenoxo ligand becomes antiferromagnetic (Table 5).

These results clearly show the existence of a counter-complementary effect[46,47] between the bridging ligands accounting for the J_1 and J_2 exchange couplings in **1a** and **1b**. Thus, despite that the phenoxo or carbonato-bridged models show an expected antiferromagnetic coupling, the inclusion of the NCN bridge results in net ferromagnetism. This effect can be understood by analyzing the energy gap of singly occupied molecular orbitals (SOMOs): the presence of all of the bridging ligands reduce the energy gap, leading to a moderate ferromagnetic coupling in agreement with the Hay−Thibeault−Hoffmann model.[48] These results for the dinuclear models also confirm the slight role of the carbonato bridging ligand in the J_2 exchange coupling. This is an expected fact, considering the relatively long Cu−O axial bond distances (between 2.09 and 2.12 Å).

The spin density distribution for the complexes **1a** and **1b** is shown in Figure 6. The main mechanism is the delocalization, logically considering the electronic configuration of the Cu(II) cation bearing the unpaired electron in M−L antibonding orbitals.[49] There is not significant negative spin population in such molecules, reflecting the small role of the polarization mechanism. The spin density in the μ_2-$\eta^1\eta^1$-O,O carbonato ligand pathway is very small because of the long Cu−O axial distances, confirming the results of the models presented in Table 5, while it is considerably larger in the μ_2-η^2-O way. In the case of the J_2 interaction due to the delocalization, there is a large amount of spin population at the oxygen atom of the phenoxo bridge and at the nitrogen atoms of the NCN pathway of the Schiff base. Hence, in this case, the coupling through the phenoxo

(45) Ruiz, E.; Alemany, P.; Alvarez, S.; Cano, J. *Inorg. Chem.* **1997**, *36*, 3683.
(46) Escuer, A.; Vicente, R.; Mautner, F. A.; Goher, M. A. S. *Inorg. Chem.* **1997**, *36*, 1233.
(47) Gutierrez, L.; Alzuet, G.; Real, J. A.; Cano, J.; Borras, J.; Castiñeiras, A. *Inorg. Chem.* **2000**, *39*, 3608.
(48) Hay, P. J.; Thibeault, J. C.; Hoffmann, R. *J. Am. Chem. Soc.* **1975**, *97*, 4884.
(49) Cano, J.; Ruiz, E.; Alvarez, S.; Verdaguer, M. *Comments Inorg. Chem.* **1998**, *20*, 27.

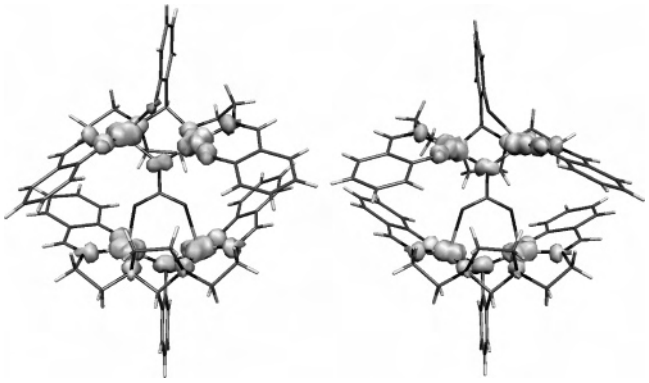

Figure 6. Representation of the spin density maps calculated a B3LYP level for the quintet ground state of the two tetranuclear complexes **1a** (left)- and **1b** (right). Clear and dark regions indicate positive and negative spin populations, respectively.

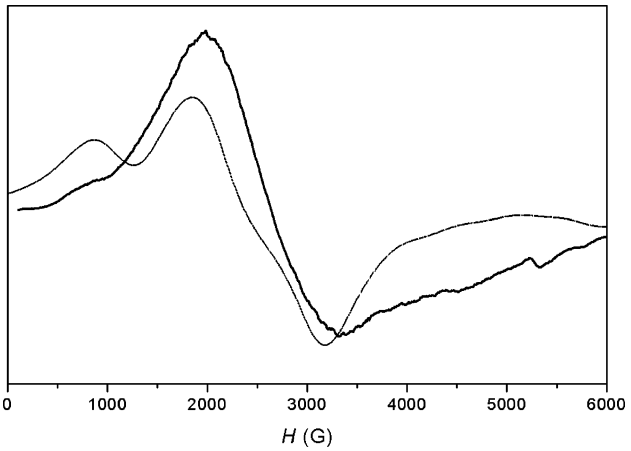

Figure 7. Solid EPR spectrum of **1**·8H_2O at 5 K (solid line), and simulated EPR spectra for a $S = 2$ state, with $D = 0.42$ cm^{-1}, $g_\perp = 2.2$, $g_{||} = 2.0$, and bandwidth = 500 G (dashed line).

bridging ligand is important, while for the J_1 interaction does not play a significant role, because of one large Cu−O bond distance.

EPR Spectra. The EPR spectrum of **1**·8H_2O at room temperature shows two bands, despite the low response observed: a small band around 900 G and a broad band about 3200 G ($\Delta H_{p-p} = 1400$ G). A more intense spectrum was obtained at low temperature (5 K) (Figure 7) with a similar form, a shoulder at 800 G and a very broad band centered at 2600 G.

With the aim to see if this spectrum is due to the $S = 2$ ground state or to the superimposition of the spectra of different spin states, the energy of the different spin states has been calculated, with the three sets of J values (Figure 8). Despite the fact that the energy values are very sensitive to relatively small changes in the J values, the first gap $\Delta = |E_{S=2} - E_{S=1}|$ is similar for the three sets of parameters: with the parameters of **1a**, $\Delta = 1.41$ cm^{-1}, with the parameters of **1b**, $\Delta = 2.04$ cm^{-1}, and with the parameters of the fit, $\Delta = 1.76$ cm^{-1}, an intermediate value. In the same way, the population of each spin state, calculated with the expression $P_S = (2S + 1)\exp(-E_S/kT)/[\Sigma(2S + 1)\exp(-E_S/kT)]$, is very close in the three cases, with intermediate values using the E_S obtained after the fit.

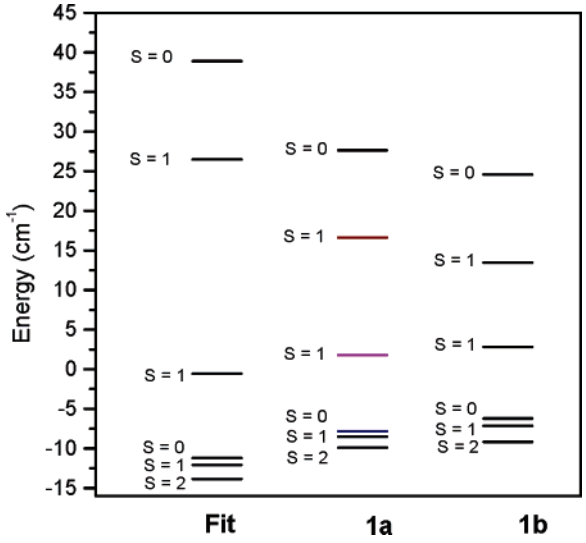

Figure 8. Energy of the spin state calculated using a different set of parameters. Fit: $J_1 = 12.42$ cm^{-1}, $J_2 = 39.44$ cm^{-1}, $J_3 = 0.50$ cm^{-1}, and $J_4 = -1.26$ cm^{-1}. Calculated values for **1a**: $J_1 = 11.0$ cm^{-1}, $J_2 = 25.8$ cm^{-1}, $J_3 = 0.11$ cm^{-1}, and $J_4 = 1.3$ cm^{-1}. Calculated values for **1b**: $J_1 = 11.1$ cm^{-1}, $J_2 = 21.5$ cm^{-1}, $J_3 = -0.06$ cm^{-1}, and $J_4 = 2.1$ cm^{-1}.

The most populated state is the $S = 2$ (0.68, at 5 K), but there is also an important population in the $S = 1$ state (0.25), with the population of the $S = 0$ spin state (0.064) being considerably lower. The found E_S values with the corrected parameters are $P_2 = 0.65$ (**1a**), 0.69 (**1b**), $P_1 = 0.26$ (**1a**), 0.24 (**1b**), and $P_0 = 0.072$ (**1a**), 0.060 (**1b**). Then, the ground state $S = 2$ is not isolated in this compound.

Consequently, the observed broad spectrum could be explained by the presence of several spin states populated at low temperature and also be due to the presence of zero field splitting. The spectrum at 5 K can be reasonably simulated with Weihe's program[29] considering an isolated $S = 2$ state (the most populated one at low temperature). Acceptable agreement between the experimental and simulated spectrum is obtained with a zero field splitting parameter $D = 0.42$ cm^{-1}, $E = 0.02$ cm^{-1}, and g values of $g_\perp = 2.2$ and $g_{||} = 2.0$ (Figure 7 dotted line). However, the simulation does not exactly reproduce the experimental spectrum, as could be expected taking into account that the $S = 1$ spin state is also populated.

Conclusions

This paper describes a simple route to isolate the tetranuclear complex [$(Cu_2L)_2(CO_3)$] (**1**), by self-assembly of dinuclear units and adventitious carbon dioxide. The crystal structure of the complex presents some unusual features, as the miscellaneous coordination polyhedra around the metal centers. In addition, the magnetic characterization shows an unexpected overall ferromagnetic coupling, which is highly unfamiliar for this type of complex. DFT calculations allow the assignment of the coupling constants to specific interactions and prove that the NCN bridging moiety of the Schiff base ligand plays a fundamental role in the observed magnetic behavior. Consequently, it seems that this kind of ligand favors ferromagnetism. This is a remarkable finding

as it is well-known that an important hindrance for the development of the field of molecular magnetism is the scarcity of bridging ligands that promote ferromagnetic coupling in di- or polynuclear transition metal complexes.

Acknowledgment. The authors thank Xunta de Galicia (PGIDT03XIB20901PR) and Ministerio de Ciencia y Tecnologia (BQ2003-00538 and BQU2002-04033-C02-02) for financial support. The computing resources were generously made available in the Centre de Computació de Catalunya (CESCA) with a grant provided by Fundació Catalana per a la Recerca (FCR) and the Universitat de Barcelona.

Supporting Information Available: Crystallographic data for complex **1**·$6H_2O$ in CIF format and Figure S1. This material is available free of charge via the Internet at http://pubs.acs.org.

IC0482741